Inverse Problems, Design and Optimization Symposium
Rio de Janeiro, Brazil, 2004

INVERSE PROCEDURE FOR PARAMETERS IDENTIFICATION OF CONTINUUM DAMAGE MODELS

Cecilia Iacono and Lambertus J. Sluys
Faculty of Civil Engineering and Geosciences,
Delft University of Technology
Delft, The Netherlands
c.iacono@citg.tudelf.nl and l.j.sluys@.citg.tudelft.nl

Jan G. M. van Mier
Institute for Building Materials
ETH Hönggerberg
Zürich, Switzerland
vanmier@ibwk.baug.ethz.ch

ABSTRACT

The parameter identification problem of the gradient-enhanced continuum damage model is presented as optimization problem.

The experimental results of tensile size effect tests on concrete specimens are used for the evaluation of the error between the experimental and computational data that has to be minimized.

Important issues are analyzed: the parameters identifiability in relation with the experimental information involved in the inverse problem, the influence of the initial guess of the model parameters on their final estimates, the limits of the model in reproducing the experimental size effect curve of tests that are strongly statistical.

INTRODUCTION

Fracture phenomena in quasi-brittle materials may be described by discrete or continuum models. In the first type of models the failure of the mechanical system is reproduced by definition of a fracture criterion along the crack and linear elastic relations in the remaining part. In the continuum models, instead, the loss of mechanical integrity is accounted for in the constitutive relations. A zone of material degradation and localized deformation, according to the standard continuum mechanics theory, represents the fracture.

However, the reliability and the predictive capacity of both classes of models rely on the correct estimation of the model parameters. These parameters may not all be directly measurable in the laboratory and an inverse problem has to be solved.

The paper presents the parameter identification problem of the elasticity based gradient-enhanced continuum damage model that belongs to the second class of models described above.

The model is briefly presented in the next Section, followed by the formulation of the inverse problem and some applications (see also [10]).

GRADIENT-ENHANCED DAMAGE MODEL (FORWARD PROBLEM)

Local formulation

The adopted numerical model is based on the isotropic continuum damage formulation of Lemaitre and Chaboche [1].

A scalar invariant measure of strain, the equivalent strain ε_{eq}, is defined as function of the strain tensor components. Different definitions of ε_{eq} can be formulated. Here the following modified von Mises definition [2] is adopted:

$$\varepsilon_{eq} = \frac{(\eta-1)I'_1}{2\eta(1-2\nu)} + \frac{1}{2\eta}\sqrt{\frac{(\eta-1)^2 I'^2_1}{(1-2\nu)^2} + \frac{12\eta J'_2}{(1+\nu)^2}} \quad (1)$$

where I_1' and J_2' are the first invariant of the strain tensor and the second invariant of the deviatoric strain tensor, respectively, and η is a model parameter representing the ratio between the compressive and tensile strength of the material: $\eta=f_{cc}/f_{ct}$.

As long as the equivalent strain ε_{eq} is smaller than a strain threshold κ_i, no damage occurs in the material. The scalar variable representing the damage ω is equal to zero and the material behavior is linear elastic, being:

$$\boldsymbol{\sigma} = (1-\omega)\mathbf{D}_{el}\boldsymbol{\varepsilon} \quad (2)$$

where $\mathbf{D}_{el}$ is the matrix of the virgin elastic stiffness moduli.

When $\varepsilon_{eq}=\kappa_i$ the damage process starts, evolving according to the following relations:

$$\omega = 1 - \frac{\kappa_i}{\kappa}[1 - \alpha + \alpha e^{-\beta(\kappa-\kappa_i)}] \tag{3}$$

$$\kappa = \max(\varepsilon_{eq}, \kappa_{max}) \tag{4}$$

where κ_{max} is the maximum value of equivalent strain occurred in the material, and α and β are two additional model parameters.

The result is a softening curve, given by the Equation 2 and 3, where the residual stress of the damaged material (ω=1) is governed by α and the (negative) slope of the softening branch is governed by β, as schematically represented in Figure 1.

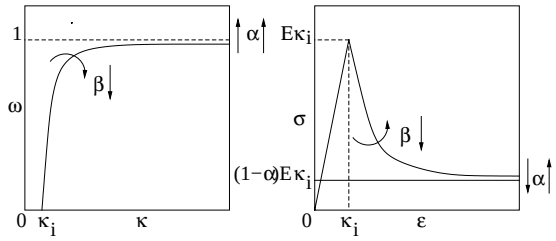

Figure 1. Exponential softening damage evolution law and uniaxial stress-strain curve.

Whether damage growth is possible is determined on the basis of a loading function:

$$f(\varepsilon_{eq}) = \varepsilon_{eq} - \kappa(\varepsilon_{eq}) \tag{5}$$

with the following Kuhn-Tucker relations:

$$f\dot{\kappa} = 0 \qquad f \le 0 \qquad \dot{\kappa} \ge 0 \tag{6}$$

However the numerical results obtained using the above formulation are affected by mesh dependence. One of the possible ways of regularizing the model is through the introduction of the concept of non-locality.

Nonlocal formulation

A nonlocal equivalent strain is introduced as a spatially averaged quantity in a neighborhood of a material point, whose size is determined by a model parameter known as the length scale [3], [4]:

$$\bar{\varepsilon}_{eq}(\boldsymbol{x}) = \frac{1}{\int_\Omega \Psi(\boldsymbol{y};\boldsymbol{x})\mathrm{d}\Omega}\int_\Omega \Psi(\boldsymbol{y};\boldsymbol{x})\varepsilon_{eq}(\boldsymbol{y})\mathrm{d}\Omega \tag{7}$$

where $\boldsymbol{y}$ points to the position of the infinitesimal volume $\mathrm{d}\Omega$. The homogeneous and isotropic Gauss distribution is usually adopted for the weight function $\Psi(\boldsymbol{y}\,;\boldsymbol{x})$.

In a gradient damage formulation the integral Equation 7 can be approximated by the following partial differential equation [5]:

$$\bar{\varepsilon}_{eq} - c\nabla^2\bar{\varepsilon}_{eq} = \varepsilon_{eq} \tag{8}$$

where $\nabla^2=\Sigma_i\partial^2/\partial x_i^2$ and c is the gradient parameter, which is related to the internal length scale parameter.

The diffusion Equation 8 has to be solved in addition to the classical equilibrium problem described previously, replacing ε_{eq} with the nonlocal counterpart $\bar{\varepsilon}_{eq}$ in the Equations 4 and 5.

All the model parameters may be collected in a vector $\mathbf{x}$:

$$\mathbf{x} = [\mathrm{E} \quad \nu \quad \kappa_i \quad \alpha \quad \beta \quad c \quad \eta]^T \tag{9}$$

where

E = Young's modulus
ν = Poisson's ratio
κ_i = strain threshold for damage initiation
α = softening curve parameter
(related to the residual stress)
β = softening curve parameter
(related to the slope of the softening branch)
c = gradient parameter
(related to the length scale parameter)
η = ratio of compressive and tensile strength f_{cc}/f_{ct}

The inverse problem consists therefore in identifying the vector $\mathbf{x}$.

PARAMETER IDENTIFICATION PROBLEM (INVERSE PROBLEM)

During laboratory tests, n_y observable quantities (e.g. forces, displacements etc.) can be measured at different "instants" t and collected in

a vector $\mathbf{y}^t_{exp}$ for t=1,2,3....n_t. On the other hand, starting from an initial guess of **x**, the same quantities may be computed solving the forward problem presented in the previous Section and collected in a corresponding vector $\mathbf{y}^t_{comp}(\mathbf{x})$. On the basis of the discrepancy between the two vectors $\mathbf{y}^t_{exp}$ and $\mathbf{y}^t_{comp}(\mathbf{x})$ a new updated estimation of **x**, depending on the adopted inverse technique, is computed. This iterative procedure, common to many inverse techniques, is implemented in a statistical context in the case of the Kalman filter method, which is used here for the applications.

Kalman filter method (KF)

The basic notions and equations of the method are presented, while for a complete treatment see e.g. [6] and [7].

The solution of the forward problem depends on the model parameter vector **x** according to the following general relation:

$$\mathbf{y}^t_{comp}(\mathbf{x}) = \mathbf{h}_t(\mathbf{x}) \tag{10}$$

where $\mathbf{h}_t(\mathbf{x})$ is the *forward operator*, that in the case of the gradient-enhanced damage model is a nonlinear operator.

The following assumptions are considered:
- the mathematical model, i.e. the forward operator $\mathbf{h}_t(\mathbf{x})$, is deterministic
- measurements uncertainties, represented by a vector $\mathbf{v}_t$, are Gaussian white noises (i.e. zero mean and $\mathbf{C}_{exp}$ covariance matrix):

$$\mathbf{y}^t_{exp} = \mathbf{y}^t_{comp}(\mathbf{x}) + \mathbf{v}_t = \mathbf{h}_t(\mathbf{x}) + \mathbf{v}_t \tag{11}$$

- an initial "a priori" estimate of the model parameter vector **x** is available, that is assumed to be statistically defined by a Gaussian distribution with mean $\mathbf{x}_0$ and covariance matrix $\mathbf{C}_0$.

Starting from those assumptions the parameter identification problem becomes the following optimization problem:

$$\hat{\mathbf{x}} = \min_{\mathbf{x}}\{(\mathbf{y}^t_{exp} - \mathbf{h}_t(\mathbf{x}))^T(\mathbf{C}^t_{exp})^{-1}(\mathbf{y}^t_{exp} - \mathbf{h}_t(\mathbf{x})) + (\mathbf{x}-\mathbf{x}_0)^T\mathbf{C}_0^{-1}(\mathbf{x}-\mathbf{x}_0)\} \tag{12}$$

In case of a nonlinear forward operator, the solution of the minimization problem represented by Equation 12 requires a step-by-step linearization (1st-order Taylor expansion) of $\mathbf{h}_t(\mathbf{x})$, obtaining the following set of equations:

$$\mathbf{L}_t = \frac{\partial \mathbf{h}_t}{\partial \mathbf{x}}(\hat{\mathbf{x}}_{t-1}, t) \tag{13}$$

$$\mathbf{K}_t = \hat{\mathbf{C}}_{t-1}\mathbf{L}_t^T[\mathbf{L}_t\hat{\mathbf{C}}_{t-1}\mathbf{L}_t^T + \mathbf{C}^t_{exp}]^{-1} \tag{14}$$

$$\hat{\mathbf{x}}_t = \hat{\mathbf{x}}_{t-1} + \mathbf{K}_t(\mathbf{y}^t_{exp} - \mathbf{h}_t(\hat{\mathbf{x}}_{t-1})) \tag{15}$$

$$\hat{\mathbf{C}}_t = \hat{\mathbf{C}}_{t-1} - \mathbf{K}_t\mathbf{L}_t\hat{\mathbf{C}}_{t-1} \tag{16}$$

where the tangent operator $\mathbf{L}_t$ is the *sensitivity matrix* and $\mathbf{K}_t$ the *gain matrix*.

Equations 13-16 define a recursive procedure that, filtering along the sequence of experimental data, gives at each step *t* a better estimate of the model parameter vector **x** and the associated covariance matrix **C**.

NUMERICAL APPLICATIONS

Experimental data

The parameter identification problem, related to the gradient-enhanced damage model, is solved using the experimental data of uniaxial tensile size effect tests. The tests, performed in the Stevinlab of the Delft University of Technology [8], concern concrete dog-bone shaped specimens of six sizes reported in Figure 2.

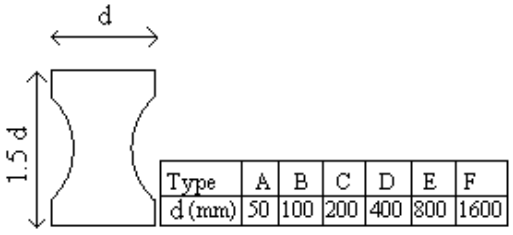

Type	A	B	C	D	E	F
d (mm)	50	100	200	400	800	1600

Figure 2. Specimen shape and dimensions for the adopted size range of the tensile size effect tests.

For computing time reasons only α, β and *c,* among all the model parameters collected in the vector **x** (see Equation 9), are involved in the identification procedure. The remaining parameters are considered as a priori known and their values, measured in standard tests, are: E=33000 [MPa], ν=0.2, κ_i=0.0001, η=14.55.

The experimental data are force-deformation curves for all the specimen sizes. The force is the total load applied to the specimen and the

deformation is the average value of all the LVDTs placed in the middle of the specimen.

Preliminary study: neighborhood function

The initialization of the iterative KF procedure represented by the Equations 13-16 (i.e. t=1) requires an initial guess $\mathbf{x}_0$ and $\mathbf{C}_0$. In case of the nonlinear forward operator $\mathbf{h}_t(\mathbf{x})$ the choice of the initial guess may have a crucial influence on the final parameters estimate.

For this purpose a preliminary insight into the objective function of the optimization problem may be useful. Here a simple method is proposed consisting in the approximated building of the following neighborhood function surface, in correspondence of a certain zone of the parameter space:

$$f(\mathbf{x}) = (\mathbf{y}_{comp}(\mathbf{x}) - \mathbf{y}_{exp})^T \mathbf{C}_{exp}^{-1} (\mathbf{y}_{comp}(\mathbf{x}) - \mathbf{y}_{exp}) \quad (17)$$

The function represented by Equation 17 represents the squared weighted distance between the two vectors $\mathbf{y}^t_{exp}$ and $\mathbf{y}^t_{comp}(\mathbf{x})$. The minimizer $\mathbf{x}$ of $f(\mathbf{x})$ corresponds to the minimum discrepancy between the experimental and numerical solution. Once a population of model parameter vectors $\mathbf{x}_i$ is chosen, with i=1,2…n_p, the neighborhood function $f(\mathbf{x}_i)$ may be evaluated for each individual and an approximation of the surface may be built. Here the selected parameters population is represented by the sets generated by all the combinations of the values given in the Table 1.

Table 1. Values for the generation of the parameters population

Parameter	c [mm^2]	β	α
Value n. 1	20.0	1500.0	0.93
Value n. 2	25.0	1400.0	0.94
Value n. 3	30.0	1300.0	0.95
Value n. 4	35.0	1200.0	-
Value n. 5	40.0	1100.0	-
Value n. 6	45.0	1000.0	-
Value n. 7	50.0	900.0	-
Value n. 8	-	800.0	-
Value n. 9	-	700.0	-

For each specimen size a total number of 7x9x3=189 forward problems is solved in order to compute the vector $\mathbf{y}^t_{comp}(\mathbf{x}_i)$ and then $f(\mathbf{x}_i)$ according Equation 17.

The quantities in the vector $\mathbf{y}^t_{comp}(\mathbf{x})$ are represented by 100 points along the global force-deformation curve. In other words, 100 forces corresponding to 100 fixed and equally spaced deformations are considered in a batch form (the superscript index t disappears in Equation 17, i.e. t=1) for the experimental-numerical comparison:

$$\mathbf{y}_{comp}(\mathbf{x}) = [F^1_{comp}(\mathbf{x}) \quad ... \quad F^{100}_{comp}(\mathbf{x})]^T \quad (18)$$

The plot of the approximated surface $f(\mathbf{x})$ as function of c and β, starting from the 189 points $f(\mathbf{x}_i)$, is shown in Figure 3 for each specimen size (type F omitted because of the large computational effort). Only the case of α=0.93 is presented, since analogous results are obtained for the other values of α.

The objective function $f(\mathbf{x})$ has basically a saddle shape. All the parameter sets corresponding to the saddle area give numerical results $\mathbf{y}^t_{comp}$ that are approximations of the same quality of the experimental data $\mathbf{y}^t_{exp}$. Additional experimental information is necessary in order to select only one model parameter set. The gradient parameter c and the softening parameter β turn out to be correlated if only global data (force-deformation curves) is considered in the solution of the inverse problem.

KF solution

Four KF identification procedures are considered, in the case of the specimen type B, in order to investigate the influence of $\mathbf{C}_0$, $\mathbf{C}_{exp}$, and the number of KF steps n_t on the final parameters estimate. The related data are reported in Table 2. In all four cases only c and β are involved in the identification procedure (α=0.95 considered as a priori known), starting from an initial guess $\mathbf{x}_0=[c_0\ \beta_0]^T=[40\ 1200]^T$.

Table 2. KF procedures data

KF proc.	$\mathbf{C}_0$ [%]	$\mathbf{C}_{exp}$ [%]	$\mathbf{n}_t$
KF_I (ref.)	40	50 (real)	20
KF_{II}	10	50	20
KF_{III}	40	5	20
KF_{IV}	40	50	30

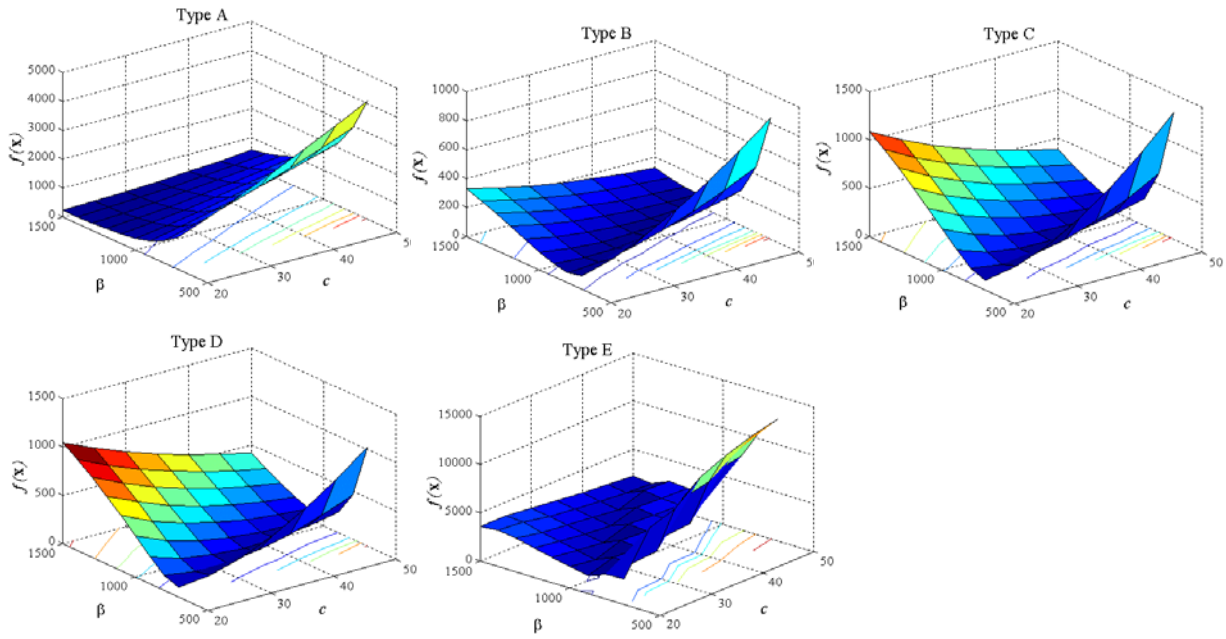

Figure 3. Neighborhood function $f(\mathbf{x})$ for different specimen sizes (α=0.93 for all cases).

The total force applied to the specimen is considered at each KF step, so that the vector $\mathbf{y}^t_{comp}(\mathbf{x})$ becomes a scalar quantity:

$$y^t_{comp}(\mathbf{x}) = F^t_{comp}(c,\beta) \tag{19}$$

The initial guess $\mathbf{x}_0$ and the final parameter estimates of the four KF procedures are reported in Figure 4. The local and global minima of the neighborhood function (Equation 17) are also shown in the same figure.

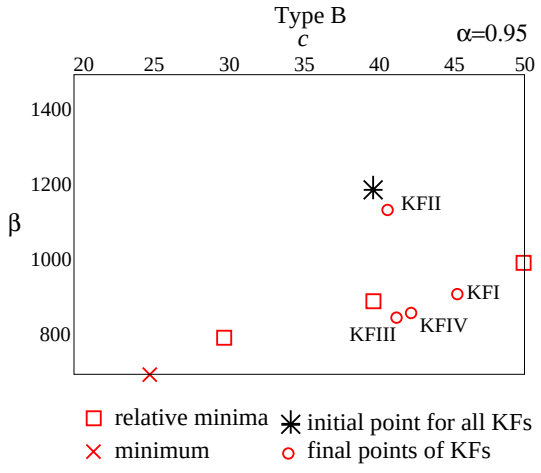

Figure 4. Estimated parameter sets for KF_I, KF_{II}, KF_{III}, KF_{IV}.

Although the neighborhood function exploits the experimental force-deformation curve in a batch form (i.e. t=1) while the KF updates the parameters estimate at each t on the basis of a single point of that curve, interesting remarks can be made by a comparison in Figure 4.

- The covariance matrix $\mathbf{C}_0$ associated with $\mathbf{x}_0$ is a measure of the uncertainty on the initial guess, and the final solution remains confined within an area proportional to $\mathbf{C}_0$. Hence the final estimate computed by KF_{II}, characterized by the smallest covariance $\mathbf{C}_0$, is close to the initial guess $\mathbf{x}_0$. In fact, if an additional penalty term concerning the initial guess is introduced in the neighborhood function (Equation 17):

$$f(\mathbf{x}) = (\mathbf{y}_{comp}(\mathbf{x}) - \mathbf{y}_{exp})^T \mathbf{C}^{-1}_{exp} (\mathbf{y}_{comp}(\mathbf{x}) - \mathbf{y}_{exp}) + \\ +(\mathbf{x} - \mathbf{x}_0)^T \mathbf{C}^{-1}_0 (\mathbf{x} - \mathbf{x}_0)^T \tag{20}$$

the function $f(\mathbf{x})$ takes a convex shape related to $\mathbf{C}_0$, as shown in Figure 5. The comparison between Figure 4 and Figure 5 points out the important role of $\mathbf{C}_0$ and $\mathbf{x}_0$.

- An area of uncertainty proportional to $\mathbf{C}_{exp}$ may be defined around the mean value $\mathbf{y}^t_{exp}$. Only the numerical solutions within that area are good approximations of the experimental solution. Hence, in case of the KF_{III}, with the smallest $\mathbf{C}_{exp}$,

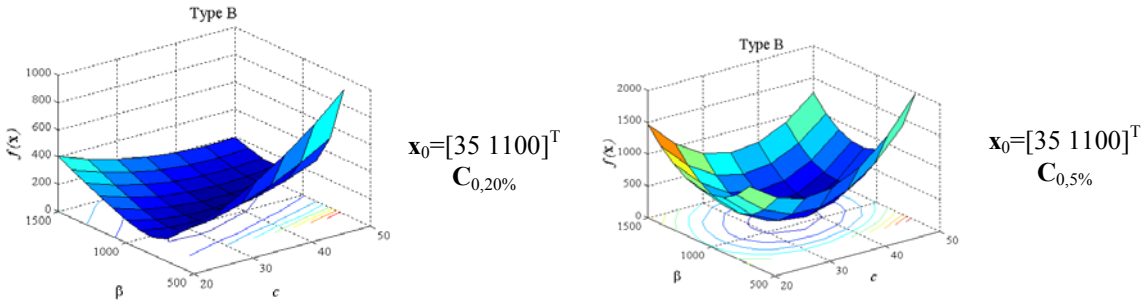

Figure 5. The effect of the initial guess $\mathbf{x}_0$ and the associated covariance $\mathbf{C}_0$ in the neighborhood function $f(\mathbf{x})$.

the final estimation $\mathbf{x}$ is forced to correspond to a numerical solution $\mathbf{y}^t_{comp}(\mathbf{x})$ close to $\mathbf{y}^t_{exp}$, approaching the local minima of the neighborhood function. If a discrepancy between the computational and the experimental curve exists, the KF performs well in minimizing this discrepancy only if a narrow strip around the experimental curve is defined by $\mathbf{C}_{exp}$ and a large strip around the computational curve is defined by $\mathbf{C}_0$ (see Figure 6).

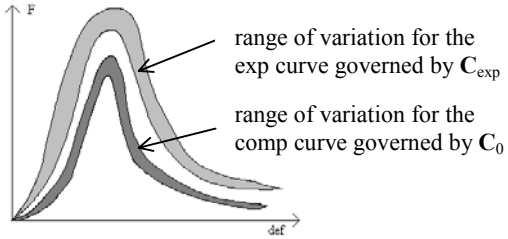

Figure 6. Meaning of $\mathbf{C}_{exp}$ and $\mathbf{C}_0$.

- The final estimation is improved by increasing the number of KF steps, as in the case of KF_{IV}.
- The parameter sets identified by the considered KF procedures converge to the same local minimum (except KF_{II}), being the starting point in that attraction basin.

Size effect curve

The plot of the peak forces versus the characteristic sizes of the specimen represents the size effect curve.

Considering only one model parameter set for all the specimen sizes, a computational curve is obtained that is too flat with respect of the experimental curve, as shown in Figure 7. Varying the set (see Figure 7) only result in a vertical shift of the curve. A possible explanation is that the considered experimental tests are characterized by a strong statistical effect: the statistical distribution of the model parameters is related to the statistical variation of local material properties in each specimen size. The adopted deterministic damage model can not capture this phenomenon [9].

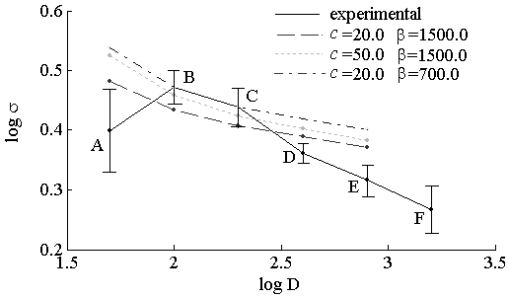

Figure 7. Experimental and computational size effect curves.

Effect of local experimental data

The effect of adding local experimental information in the definition of the neighborhood function (Equation 17) is investigated in the simple case of one-dimensional bar in tension, with a weak zone in the middle part, where deformation and damage localize.

The load-deformation curve, the damage profile and the equivalent strain profile along the bar represent the solution of the forward problem.

Pseudo-experimental data are created artificially considering analytical curves that are close to the computational curves corresponding to the following reference parameter set: $\mathbf{x} = [c\ \beta]=[30\ 1500]^T$ (see Figure 8).

The remaining model parameters, considered as a priori known, are E=20000 [MPa], ν=0.0, α=0.95, κ_i=0.0001/0.00009 (the smaller value for the weak part of the bar), η=14.00. Geometrical data are: bar length L= 100.0 [mm], length of the weak part l= 10 [mm], cross-section A= 10 [mm^2].

The neighborhood function $f(\mathbf{x})$ may be rewritten in the following form, with three separate contributions:

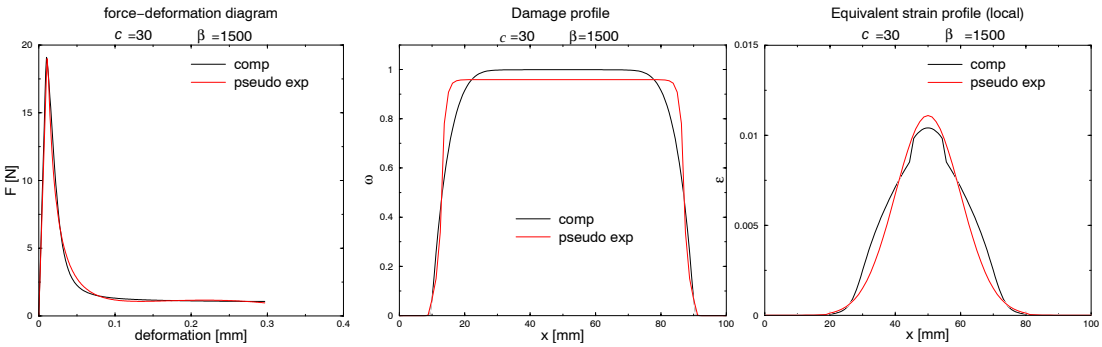

Figure 8. Pseudo-experimental data

$$f(\mathbf{x}) = \underbrace{\frac{(\mathbf{y}_{comp}(\mathbf{x}) - \mathbf{y}_{exp})^T (\mathbf{y}_{comp}(\mathbf{x}) - \mathbf{y}_{exp})}{(\mathbf{y}_{exp})^T (\mathbf{y}_{exp})}}_{1} + \underbrace{\frac{(\boldsymbol{\omega}_{comp}(\mathbf{x}) - \boldsymbol{\omega}_{exp})^T (\boldsymbol{\omega}_{comp}(\mathbf{x}) - \boldsymbol{\omega}_{exp})}{(\boldsymbol{\omega}_{exp})^T (\boldsymbol{\omega}_{exp})}}_{2} + \underbrace{\frac{(\boldsymbol{\varepsilon}_{eq,comp}(\mathbf{x}) - \boldsymbol{\varepsilon}_{eq,exp})^T (\boldsymbol{\varepsilon}_{eq,comp}(\mathbf{x}) - \boldsymbol{\varepsilon}_{eq,exp})}{(\boldsymbol{\varepsilon}_{eq,exp})^T (\boldsymbol{\varepsilon}_{eq,exp})}}_{3} \quad (21)$$

where in the vectors $\boldsymbol{\omega}$ and $\boldsymbol{\varepsilon}$ points are collected along the damage profile curve and equivalent strain profile curve, respectively.

Analogous to the previous case, a population of model parameter sets $\mathbf{x}_i$ is chosen and the approximation of the neighborhood function is built from the evaluations of $f(\mathbf{x}_i)$. The plots and contour plots of $f(\mathbf{x})$ are reported in Figure 9 considering the various contributions in Equation 21. The introduction of additional experimental information concerning the process zone (damage or strain field data) in the solution of the inverse problem is necessary for the correct estimation of the model parameter vector.

CONCLUSIONS

The Kalman filter technique is a powerful tool that identifies not only the model parameters, but also the related uncertainty. However, the non-linearity of the problem makes the choice of the initial guess $\mathbf{x}_0$ and the associated covariance matrix $\mathbf{C}_0$ a crucial factor with significant influence on the final parameters estimate. A preliminary study of the objective function is useful for the selection of the initial guess and in order to have insight in the well posedness of the inverse problem.

In case of the gradient-enhanced continuum damage model, the parameter identification problem based only on the global experimental information of the force-displacement curve lacks an unique solution: a correlation is found between the gradient parameter c and the softening parameter β. Additional experimental information, related to the strain or damage distribution in the failure process zone, is necessary for a correct estimation of the model parameters.

The examined numerical model, with only one model parameter set, can not reproduce the experimental size effect curve of the considered dog-bone shaped specimens, due to the strong statistical characteristic of the tests.

ACKNOWLEDGEMENTS

The program related to the implementation of the gradient-enhanced model in the framework of the finite element code FEAP was kindly supplied by A. Simone.

The authors like to acknowledge M. R .A. van Vliet for having supplied the experimental results and the Technical Science Foundation in the Netherlands (STW) for financial support to CI.

REFERENCES

1. J. Lemaitre and J. L. Chaboche, *Mechanics of Solids Material*, Cambridge University Press, Cambridge, 1990.

2. J. H. P. Vree, W. A. M. Brekelmans and M. A. J. Gils, Comparison of nonlocal approaches in continuum damage mechanics, *Computers and Structures*, **55**, 581-588 (1995).

3. Z. P. Bažant and G. Pijaudier-Cabot, Nonlocal continuum damage, localization instability and convergence, *Journal of Applied Mechanics*, **55**, 287-293, (1988).

4. G. Pijaudier-Cabot and Z. P. Bažant, Nonlocal damage theory, *ASCE Journal of Engineering Mechanics* **113** (10), 1512-1533, (1987).

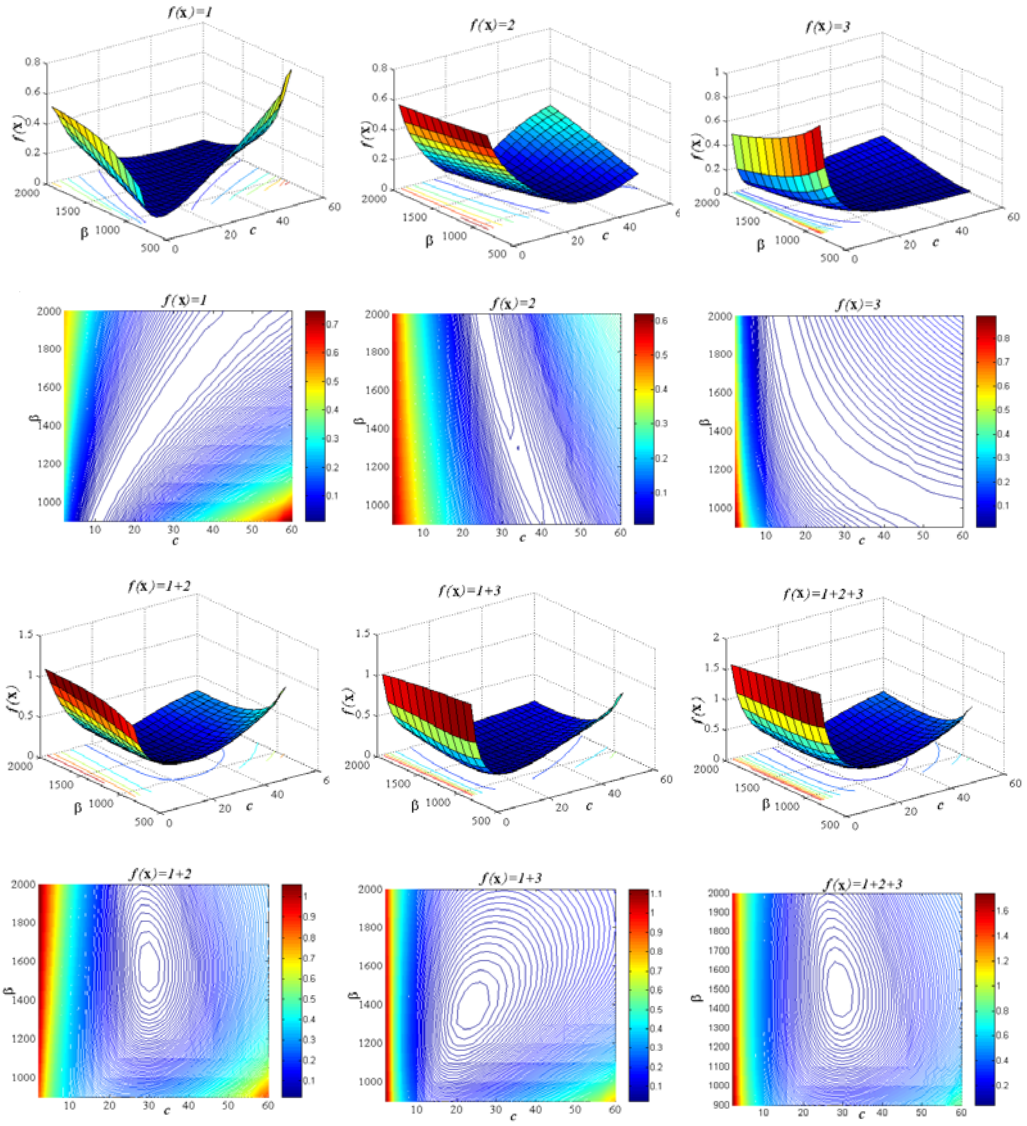

Figure 9. Neighborhood function $f(\mathbf{x})$ considering different experimental information contribution (α=0.95).

5. R. H. J. Peerlings, R. de Borst, W. A. M. Brekelmans and J. H. P. de Vree 1996, Gradient-enhanced damage for quasi-brittle materials, *International Journals for Numerical Methods in Engineering,* **39**, 3391-3403, (1996).

6. S. Bittanti, G. Maier and A. Nappi, *Inverse problem in structural elastoplasticity: a Kalman filter approach*, A. Sawczuk & G. Bianchi (eds.), Plasticity Today: 311-329, Elsevier Applied Science Publ., London, 1984.

7. A. Tarantola, *Inverse Problem Theory. Methods for Data Fitting and Model Parameter estimation*, Elsevier Applied Science, Southampton, 1987.

8. M. R. A. van Vliet and J. G. M. van Mier, Experimental investigation of size effect in concrete under uniaxial tension, *Int. Conf. FraMCoS-3*, Gifu, Japan, 1998. Aedificatio Publishers, Freiburg, Germany, 1998.

9. D. Lehký and D. Novák, Modeling of size effects in concrete under uniaxial tension. *4th International Ph.D. Symposium in Civil Engineering*, Munich, Germany, vol. 1, ISBN 3-935065-09-4, pp. 435-444, 2002.

10. C. Iacono, L. J. Sluys and J. G. M. van Mier, Parameter identification of computational fracture models, *Int. Conf. FraMCoS-5*, Colorado, USA, 2004.